

# Electromagnetic Form Factors of the Nucleon in Chiral Soliton Models

G. Holzwarth

*Fachbereich Physik, Universität Siegen, D-57068 Siegen, Germany*

In this talk we give a simple and transparent argument for the characteristic decrease of the ratio  $G_E^p/G_M^p$  which arises naturally in chiral soliton models. We present a new fit within the minimal  $\pi - \rho - \omega$  model using the same interpolating powers  $n = 2$  for both, electric and magnetic form factors, for the boost to the Breit frame. The results show a significant discrepancy with data for  $G_M^n$  for  $Q^2 > 1 \text{ (GeV/c)}^2$ . We comment on the possibility to extract information about the timelike region and for two-photon amplitudes from soliton models.

## A. Introduction

In the past few years there have been no essential new theoretical developments in the results for electromagnetic nucleon form factors obtained within the framework of chiral soliton models. Electron-nucleon scattering experiments that measure ratios of polarization variables have confirmed that with increasing momentum transfer  $Q^2 = -q_\mu q^\mu$  the proton electric form factor  $G_E^p(Q^2)$  decreases significantly faster than the proton magnetic form factor  $G_M^p(Q^2)$ . This characteristic feature of the electric proton form factor arises naturally in chiral soliton models of the nucleon and has been predicted previously from such models [1],[2]. In the next section we give a very simple and transparent argument for the origin of this result.

We then present detailed results from the minimal  $\pi$ - $\rho$ - $\omega$ -meson model, where, in contrast to our previous work, we now use the same interpolating powers  $n_M = n_E = 2$  for boosting electric and magnetic form factors to the Breit frame, to enforce superconvergence for  $Q^2 \rightarrow \infty$ . The prediction for the magnetic neutron form factor  $G_M^n(Q^2)$  still seems to be in conflict with existing older data, as it consistently rises above the magnetic proton form factor for  $Q^2 > 1 \text{ (GeV/c)}^2$ .

Prospects to obtain results from soliton models for form factors in the timelike region are briefly discussed.

Finally, leading contributions to the  $2\gamma$ -exchange amplitudes in soliton models are outlined, which may help to remove the discrepancies between form factors extracted via Rosenbluth separation, and those obtained from ratios of polarization observables.

## B. Characteristic feature of the electric proton form factor

Chiral soliton models for the nucleon naturally account for a characteristic decrease of the ratio  $G_E^p/(G_M^p/\mu_p)$  with increasing  $Q^2$ . The reason for this behavior basically originates in the fact that isospin for baryons is generated by rotating the soliton in isospace. The hedgehog structure of the soliton couples the isorotation to a spatial rotation. Therefore, in the rest frame of the soliton, the isovector ( $I = 1$ ) form factors measure the (rotational) inertia density  $B_1(r)$ , as compared to the isoscalar baryon density  $B_0(r)$  for the isoscalar ( $I = 0$ ) form factors. This becomes evident from the explicit form of the isoscalar and isovector form factors in the simple purely pionic soliton model [3]:

$$G_E^0(k^2) = \frac{1}{2} \int d^3r j_0(kr) B_0(r) \quad (1)$$

$$G_M^0(k^2)/\mu_0 = \frac{3}{r_B^2} \int d^3r r^2 \frac{j_1(kr)}{kr} B_0(r) \quad (2)$$

$$G_E^1(k^2) = \frac{1}{2} \int d^3r j_0(kr) B_1(r) \quad (3)$$

$$G_M^1(k^2)/\mu_1 = 3 \int d^3r \frac{j_1(kr)}{kr} B_1(r), \quad (4)$$

(with mean square isoscalar baryon radius  $r_B^2$ , isoscalar and isovector magnetic moments  $\mu_0, \mu_1$ , and normalization  $\int B_0(r) d^3r = \int B_1(r) d^3r = 1$ ). Evidently, if the inertia density were obtained from rigid rotation of the baryon density  $B_1(r) = (r^2/r_B^2) B_0(r)$ , the normalized isoscalar and isovector magnetic form factors would satisfy the scaling relation

$$G_M^1(k^2)/\mu_1 = G_M^0(k^2)/\mu_0. \quad (5)$$

while for the electric form factors the same argument leads to

$$G_E^1(k^2) = -\frac{1}{r_B^2} \left( \frac{\partial}{\partial k} \right)^2 G_E^0(k^2). \quad (6)$$

For a Gaussian baryon density  $B_0(r)$  the 'scaling' property (5) includes also the isoscalar electric form factor

$$G_M^1(k^2)/\mu_1 = G_M^0(k^2)/\mu_0 = 2G_E^0(k^2), \quad (7)$$

and eq.(6) then leads to

$$G_E^1(k^2) = \left( 1 - \frac{1}{9} k^2 r_B^2 \right) G_E^0(k^2). \quad (8)$$

Therefore, for proton form factors

$$G_{E,M}^p = G_{E,M}^0 + G_{E,M}^1, \quad (9)$$

the ratio  $G_E^p/(G_M^p/\mu_p)$  resulting from eqs.(5), (7) and (8), is

$$R(k^2) = G_E^p(k^2)/(G_M^p(k^2)/\mu_p) = \left( 1 - \frac{1}{18} k^2 r_B^2 \right). \quad (10)$$

With  $r_B^2 \approx 2.3 \text{ (GeV/c)}^{-2} \approx (0.3 \text{ fm})^2$ , this simple consideration provides an excellent fit (see fig.3) through the polarization data for  $R(k^2)$ . Of course, in typical soliton models  $B_1(r)$  is not exactly proportional to  $r^2 B_0(r)$  and the baryon density is not really Gaussian (cf. fig.1). Furthermore, to compare with experimentally extracted form factors, the  $k^2$ -dependence of the form factors in the soliton rest frame must be subject to the Lorentz boost from the rest frame to the Breit frame (which compensates for the fact that typical baryon radii obtained in soliton models are near 0.5 fm).

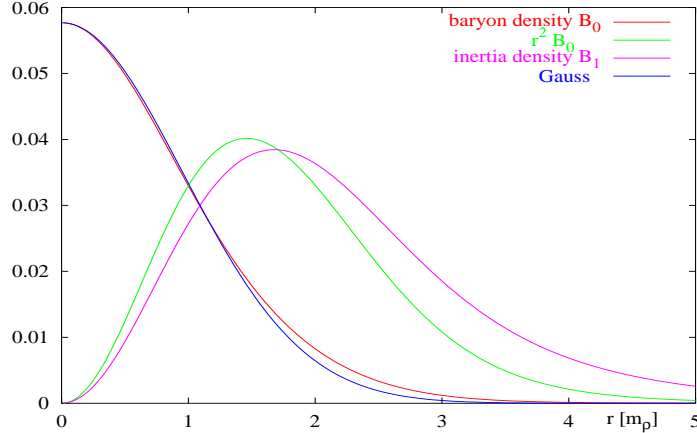


FIG. 1: Comparison between the topological baryon density  $B_0$  and a Gaussian, and between the inertia density  $B_1$  and  $r^2 B_0$ , for the standard pionic Skyrme model (11),(12) with  $e = 4.25$ .

But still, we may conclude from the above simple considerations that a strong decrease of the ratio (10) from  $R = 1$  towards an eventual zero near  $k^2 \sim 10 \text{ (GeV/c)}^2$  appears as a natural and characteristic feature of e.m. proton form factors in chiral soliton models.

### C. Chiral $\pi$ - $\rho$ - $\omega$ -meson model

After the above rather general remarks we consider a specific realistic model which includes also vector mesons. They are known to play an essential role in the coupling of baryons to the electromagnetic field and different possibilities

for their explicit inclusion in a chirally invariant effective meson theory have been suggested [4]. We adopt the pionic Skyrme model for the chiral SU(2)-field  $U$

$$\mathcal{L}^{(\pi)} = \mathcal{L}^{(2)} + \mathcal{L}^{(4)} \quad (11)$$

$$\mathcal{L}^{(2)} = \frac{f_\pi^2}{4} \int (-tr L_\mu L^\mu + m_\pi^2 tr(U + U^\dagger - 2)) d^3x, \quad \mathcal{L}^{(4)} = \frac{1}{32e^2} \int tr[L_\mu, L_\nu]^2 d^3x \quad (12)$$

( $L_\mu$  denotes the chiral gradients  $L_\mu = U^\dagger \partial_\mu U$ , the pion decay constant is  $f_\pi=93$  MeV, and the pion mass  $m_\pi=138$  MeV). Without explicit vector mesons the Skyrme parameter  $e$  is well established near  $e=4.25$ . The coupling to the photon field is obtained through the local gauge transformation  $U \rightarrow e^{i\epsilon \hat{Q}} U e^{-i\epsilon \hat{Q}}$  with the charge operator  $\hat{Q} = (\frac{1}{3} + \tau_3)/2$ . The isoscalar part of the coupling arises from gauging the standard Wess-Zumino term in the SU(3)-extended version of the model.

Vector mesons may be explicitly included as dynamical gauge bosons. In the minimal version the axial vector mesons are eliminated in chirally invariant way [5, 6, 7]. This leaves two gauge coupling constants  $g_\rho, g_\omega$  for  $\rho$ - and  $\omega$ -mesons,

$$\mathcal{L} = \mathcal{L}^{(\pi)} + \mathcal{L}^{(\rho)} + \mathcal{L}^{(\omega)} \quad (13)$$

$$\mathcal{L}^{(\rho)} = \int \left( -\frac{1}{8} tr \rho_{\mu\nu} \rho^{\mu\nu} + \frac{m_\rho^2}{4} tr(\rho_\mu - \frac{i}{2g_\rho}(l_\mu - r_\mu))^2 \right) d^3x, \quad (14)$$

$$\mathcal{L}^{(\omega)} = \int \left( -\frac{1}{4} \omega_{\mu\nu} \omega^{\mu\nu} + \frac{m_\omega^2}{2} \omega_\mu \omega^\mu + 3g_\omega \omega_\mu B^\mu \right) d^3x, \quad (15)$$

with the topological baryon current  $B_\mu = \frac{1}{24\pi^2} \epsilon_{\mu\nu\rho\sigma} tr L^\nu L^\rho L^\sigma$ , and  $l_\mu = \xi^\dagger \partial_\mu \xi$ ,  $r_\mu = \partial_\mu \xi \xi^\dagger$ , where  $\xi^2 = U$ .

The contributions of the vector mesons to the electromagnetic currents arise from the local gauge transformations

$$\rho^\mu \rightarrow e^{i\epsilon \hat{Q}_V} \rho^\mu e^{-i\epsilon \hat{Q}_V} + \frac{\hat{Q}_V}{g_\rho} \partial^\mu \epsilon, \quad \omega^\mu \rightarrow \omega^\mu + \frac{\hat{Q}_0}{g_0} \partial^\mu \epsilon \quad (16)$$

(with  $\hat{Q}_0 = 1/6$ ,  $\hat{Q}_V = \tau_3/2$ ). The resulting form factors are expressed in terms of three static and three induced profile functions which characterize the rotating hedgehog soliton with baryon number  $B = 1$ .

Because the Skyrme term  $\mathcal{L}^{(4)}$  at least partly accounts for static  $\rho$ -meson effects its strength should be reduced in the presence of dynamical  $\rho$ -mesons, as compared to the plain Skyrme model. The coupling constant  $g_\rho$  can be fixed by the KSRF relation  $g_\rho = m_\rho/(2\sqrt{2}f_\pi)$ , but small deviations from this value are tolerable. The  $\omega$ -mesons introduce two gauge coupling constants,  $g_\omega$  to the baryon current in  $\mathcal{L}^{(\rho)}$ , and  $g_0$  for the isoscalar part of the charge operator. Within the SU(2) scheme we can in principle allow  $g_0$  to differ from  $g_\omega$  and thus exploit the freedom in the e.m. coupling of the isoscalar  $\omega$ -mesons. However, as the isoscalar part of the electromagnetic current is given by the baryonic current, it is natural to expect  $g_\omega \approx g_0$ . The explicit form of the form factors (using the KSRF relation for  $g_\rho$ ) is given in [7].

#### D. Boost to the Breit frame

For all dynamical models of spatially extended clusters it is difficult to relate the non-relativistic form factors evaluated in the rest frame of the cluster to the relativistic  $Q^2$ -dependence in the Breit frame where the cluster moves with velocity  $v$  relative to the rest frame. For the associated Lorentz-boost factor  $\gamma$  we have

$$\gamma^2 = (1 - v^2)^{-1} = 1 + \frac{Q^2}{(2M)^2}, \quad (17)$$

where  $M$  is the rest mass of the cluster. For elastic scattering of clusters composed of  $n$  constituents dimensional scaling arguments [8] suggest that the leading power in the asymptotic behavior of relativistic form factors is  $\sim Q^{2-2n}$ . Boost prescriptions of the general form

$$G_M^{Breit}(Q^2) = \gamma^{-2n_M} G_M^{rest}(k^2), \quad G_E^{Breit}(Q^2) = \gamma^{-2n_E} G_E^{rest}(k^2) \quad (18)$$

with

$$k^2 = \gamma^{-2} Q^2 \quad (19)$$

have been proposed with various values for the interpolating powers  $n_M, n_E$  [9, 10], where  $M$  takes the role of an effective mass.

This boost prescription has the appreciated feature that a low- $k^2$  region in the rest frame ( $0 < k^2 < 1$  (GeV/c) $^2$ , say), where we would trust the physical content of the rest-frame form factors, appears as an appreciably extended  $Q^2$ -regime in the Breit frame. So, through the boost (19) from rest frame to Breit frame the region of validity of soliton form factors for spatial  $Q^2$  is extended.

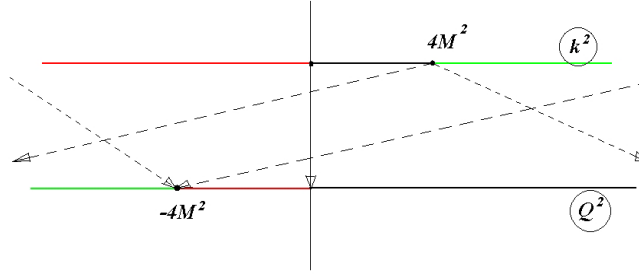


FIG. 2: The boost (19) maps the red, black, and green intervals of rest frame  $k^2$  onto the red, black, and green intervals of the Breit frame momentum transfer  $Q^2$ .

Evidently, the boost in eq.(19) maps  $G^{rest}(k^2 \rightarrow 4M^2) \rightarrow G^{Breit}(Q^2 \rightarrow \infty)$ . But, even though  $G^{rest}(4M^2)$  may be very small, it generally does not vanish exactly. So, unless  $n_M, n_E \geq 2$ , this shows up, of course, very drastically in the asymptotic behavior, if the resulting form factors are divided by the standard dipole

$$G_D(Q^2) = 1/(1 + Q^2/0.71)^2. \quad (20)$$

which is the common way to present the nucleon form factors and accounts for the proper asymptotic  $q^{2-2n}$  behavior of an  $n = 3$ -quark cluster. So it is vital for a comparison with experimentally determined form factors for  $Q^2 \gg M^2$  to employ a boost prescription which preserves at least the 'superconvergence' property  $Q^2 G(Q^2) \rightarrow 0$  for  $Q^2 \rightarrow \infty$ . In accordance with an early suggestion by Mitra and Kumari [11],[12] we use  $n_M = n_E = 2$ . In any case, the high- $Q^2$  behaviour is not a profound consequence of the model but simply reflects the boost prescription. There is no reason anyway, why low-energy effective models should provide any profound answer for the high- $Q^2$  limit. Note that the position of an eventual zero in  $G_E^{Breit}(Q^2)$  is not affected by the choice of the interpolating power  $n_E$ .

## E. Results

To demonstrate the amount of agreement with experimental data that can be achieved within the framework of such models we present in fig. 3 typical results from the  $\pi$ - $\rho$ - $\omega$ -model for the following set of parameters. With the physical values for the pion mass  $m_\pi = 138$  MeV, pion decay constant  $f_\pi = 93$  MeV,  $\rho$  and  $\omega$  masses  $m_\rho = m_\omega = 770$  MeV,  $\rho$ -coupling constant at its KSRF-value  $g_\rho = 2.9$ , there remains the  $\omega$ -coupling constant as parameter which we take at  $g_\omega = 1.3$ . Due to the presence of the  $\rho$ -mesons the strength of the Skyrme term should be reduced. We use  $e = 7.5$  for the fit shown in figs. 3 and 4. For the coupling of the  $\omega$ -mesons to the photons we use  $g_\omega = 0.85g_0$ . The effective boost mass is taken as  $M = 1.25$  GeV. Evidently, the model is able to reproduce the essential features of electromagnetic nucleon form factors.

The shape of  $G_E^n$  deviates from the Galster parametrization in a characteristic way, as its maximum is shifted to lower  $Q^2$ . The reason lies in the values for the electric neutron square radii which exceed the experimental value by about a factor of 2 and which we find difficult to lower for reasonable parametrizations within the  $SU(2)$  framework. In Table 1 we list the quadratic radii and magnetic moments as they arise from the fit given above. Notoriously low are the magnetic moments, as is well known in chiral soliton models. Quantum corrections may partly be helpful in this respect (see [13]), as they certainly are for the absolute values of the masses. In the  $SU(3)$ -extended version the strangeness content of the nucleon represented by kaonic contributions to the isoscalar and isovector charge radii may lead to a sizeable reduction of the electric neutron square radius [14].

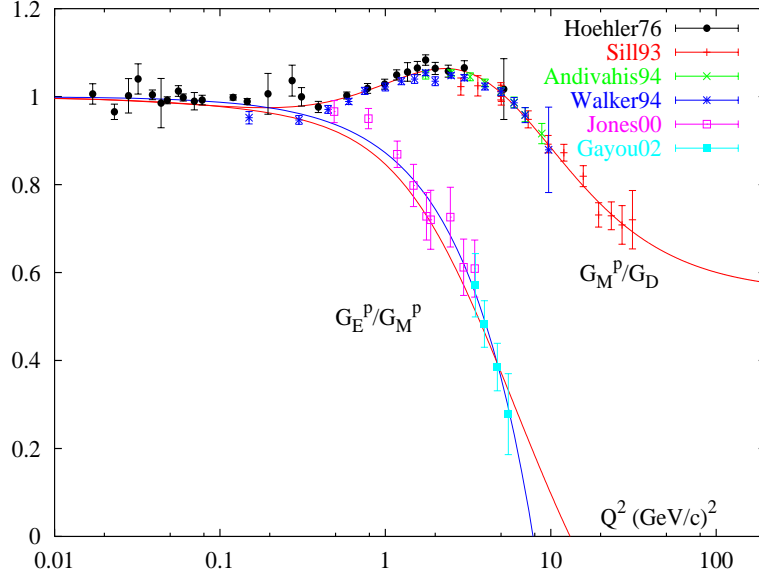


FIG. 3: Magnetic and electric proton form factors  $G_M^p/(\mu_p G_D)$  and  $G_E^p \mu_p / G_M^p$  for the  $\pi$ - $\rho$ - $\omega$ -model with the set of parameters given in the text (red lines). The blue line shows the result of equation (10) with  $r_B = 0.3$  fm. The abscissa shows  $Q^2(\text{GeV}/c)^2$  on logarithmic scale. The experimental data are from [15]-[20].

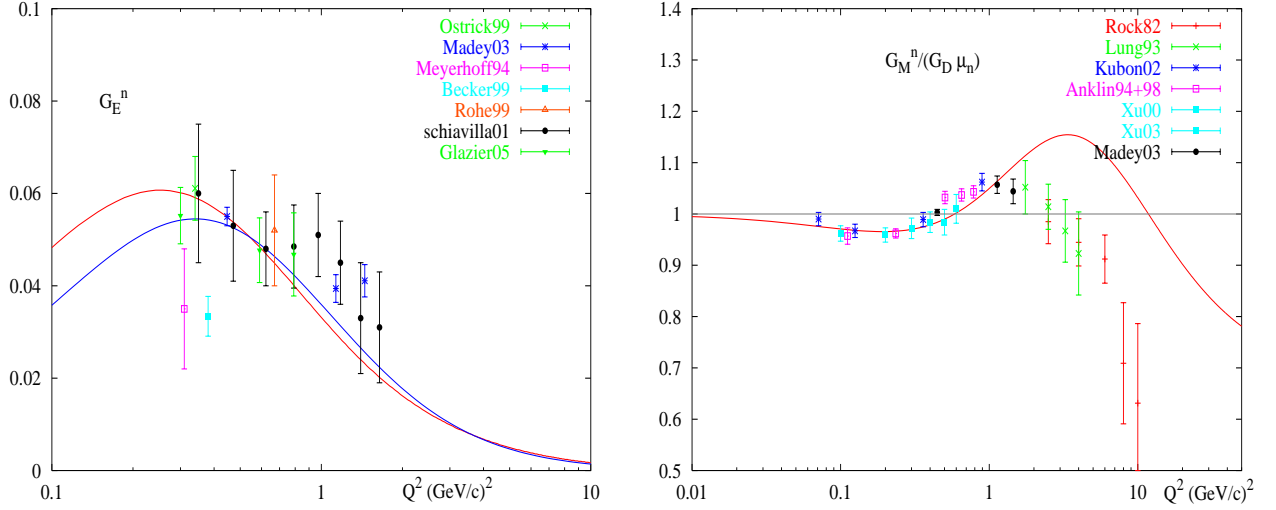


FIG. 4: The left figure shows the neutron electric form factor  $G_E^n$  as obtained in the  $\pi$ - $\rho$ - $\omega$ -model with the set of parameters given in the text. The blue line is the standard Galster parametrization  $G_E^n = 0.54Q^2/(1 + 1.54Q^2) \cdot G_D$ . Experimental results for  $G_E^n$  are mainly from more recent polarization data [21]-[27]. The right figure shows the magnetic neutron form factor (normalized to the standard dipole)  $G_M^n/(\mu_n G_D)$  in the same model. Here the data are from [27]-[34].

In Fig.4 we also present the magnetic neutron form factor  $G_M^n$ , normalized to the standard dipole  $G_D$ . For  $Q^2 \leq 1(\text{GeV}/c)^2$  the model result is in almost perfect agreement with the newer data [27],[30]-[34]. For  $Q^2 > 1(\text{GeV}/c)^2$ , however, the available older data [28, 29] deviate substantially from the model prediction. The ratio of the normalized proton and neutron form factors  $G_M^n \mu_p / (G_M^p \mu_n)$  is independent of the choice of the interpolating power  $n_M$  in the boost prescription. Therefore it would be desirable to compare directly with data for this ratio. Experimentally it is accessible from quasielastic scattering on deuterium with final state protons and neutrons detected. The model consistently predicts this ratio to increase above 1 by up to 20% for  $1 < Q^2(\text{GeV}/c)^2 < 10$ . The presently available data do not show such an increase for the ratio  $G_M^n \mu_p / (G_M^p \mu_n)$ , in fact they indicate the opposite tendency.

This conflict was already noticed in [2],[35]. Preliminary new data from CLAS<sup>++</sup> [36] presented at this meeting apparently are compatible with  $G_M^n/(G_D\mu_n) = 1$  in the region  $1.0 < Q^2(\text{GeV}/c)^2 < 4.5$ .

Of course, such models can be extended; addition of higher-order terms in the Skyrme lagrangian, explicite inclusion of axial vector mesons provide more flexibility through additional parameters. It is, however, remarkable that a minimal version as described above is able to provide the characteristic features for both proton and the electric neutron form factors in such detail, in a single model approach. In fact, the unexpected decrease of  $G_E^p$  was predicted by these models, and it will be interesting to compare with new data for  $G_M^n$  concerning the conflict indicated in Fig.4.

	$\langle r^2 \rangle_E^p$	$\langle r^2 \rangle_M^p$	$\langle r^2 \rangle_E^n$	$\langle r^2 \rangle_M^n$	$\mu_p$	$\mu_n$
Model	0.75	0.72	-0.22	0.75	1.78	-1.36
Exp.	0.77	0.74	-0.114	0.77	2.79	-1.91

TABLE I: Nucleon quadratic radii and magnetic moments as obtained from the chiral  $\pi$ - $\rho$ - $\omega$ -model, for the parameters given in the text. The experimental values are from [37].

### F. Extension to timelike $Q^2$

In the soliton restframe the extension to timelike  $k^2$  amounts to finding the spectral functions  $\Gamma(\nu^2)$  as Laplace transforms of the relevant densities  $B(r)$ , e.g. for the isoscalar electric case

$$rB_0(r) = \frac{1}{\pi^2} \int_{\nu_0^2}^{\infty} \exp^{-\nu r} \nu \Gamma_0(\nu^2) d\nu, \quad (21)$$

and similarly for other cases. In soliton models the densities are obtained numerically on a spatial grid, therefore the spectral functions cannot be determined uniquely. Results will always depend on the choice of constraints which have to be imposed on possible solutions. But with reasonable choices it seems possible to stabilize the spectral functions in the regime from the 2- or 3-pion threshold to about two  $\rho$ -meson masses and distinguish continuous and discrete structures in this regime [2].

We note (cf. fig.(2)) that the transformation to the Breit frame (19) formally maps the rest-frame form factors  $G^{rest}(k^2)$  for the whole timelike regime  $-\infty < k^2 < 0$  onto the Breit-frame form factors  $G^{Breit}(Q^2)$  in the unphysical timelike regime up to the nucleon-antinucleon threshold  $-4M^2 < Q^2 < 0$ . On the other hand, the physical timelike regime  $-\infty < Q^2 < -4M^2$  in the Breit frame is obtained as the image of the spacelike regime  $4M^2 < k^2 < \infty$  of form factors in the rest frame. So the (real parts) of the Breit-frame form factors for timelike  $Q^2$  beyond the nucleon-antinucleon threshold are formally fixed through eq.(18). However, apart from the probably very limited validity of the boost prescription (18), we do not expect that the form factors in the soliton rest frame for  $k^2 > 4M^2$  contain sufficiently reliable physical information. Specifically, oscillations which the rest-frame form factors may show for  $k^2 \rightarrow \infty$  are squeezed by the transformation (19) into the vicinity of the physical threshold  $Q^2 < -4M^2$ . With  $G^{rest}(k^2) \rightarrow 0$  for  $k^2 \rightarrow \infty$ , the Breit-frame form factors are undetermined at threshold  $Q^2 \rightarrow -4M^2$ .

Attempts to obtain form factors for timelike  $Q^2$  from soliton-antisoliton configurations in the baryon number  $B = 0$  sector face the difficulty that in this sector the only stable classical configuration is the vacuum. So, any result will reflect the arbitrariness in the construction of nontrivial configurations.

Altogether we conclude, that presently we see no reliable way for extracting profound information about e.m. form factors in the physical timelike region from soliton models.

### G. Two-photon amplitudes in soliton models

The discrepancies between form factors extracted through the Rosenbluth separation from unpolarized elastic scattering data [38] and ratios directly obtained from polarization transfer measurements [19, 20] have shifted the theoretical focus to the two-photon amplitudes which enter the unpolarized cross section and polarization variables in different ways. The problem with two-photon exchange diagrams is that they involve the full response of the nucleon

to doubly virtual Compton scattering and therefore strongly rely on nucleon models. Again it turns out that soliton models provide a comparatively simple answer for the structure of leading terms.

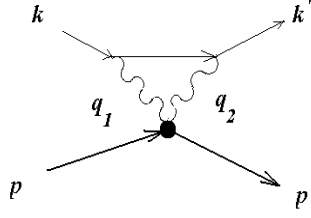


FIG. 5: Electron-nucleon scattering  $2\gamma$ -exchange amplitude with local  $2\gamma$ -soliton vertex with momentum transfer  $q = q_1 - q_2 = k - k' = p' - p$ .

Products of covariant derivatives

$$D_\mu U = \partial_\mu U + i[\hat{Q}, U]A_\mu \quad (22)$$

which appear in all terms of the derivative expansion after gauging the chiral fields with the electric charge  $\hat{Q}$ , naturally produces a number of *local* two-photon couplings, the simplest ones stemming from the quadratic nonlinear  $\sigma$ -term and from the gauged Wess-Zumino anomalous action

$$\mathcal{L}_{nl\sigma}^{(2\gamma)} = -\frac{f_\pi^2}{4} A_\mu A^\mu 2\text{tr}(\hat{Q}U\hat{Q}U^\dagger - \hat{Q}^2), \quad (23)$$

$$\mathcal{L}_{WZ}^{(2\gamma)} = i\frac{N_c}{48\pi^2} 4\epsilon^{\mu\nu\rho\sigma}(\partial_\mu A_\nu)A_\rho \text{tr}(\hat{Q}\partial_\sigma U\hat{Q}U^\dagger). \quad (24)$$

After quantization of the collective coordinates the matrix elements of these  $2\gamma$ -vertices sandwiched between incoming and outgoing nucleon states are obtained, without additional parameters, with form factors fixed through the soliton profiles. Then the interference terms with the single-photon-exchange amplitudes which enter the unpolarized elastic cross section can be evaluated, again conveniently in the Breit frame. It turns out that the contribution from  $\mathcal{L}_{nl\sigma}^{(2\gamma)}$  interferes only with the electric part of the 1-photon-exchange Born term and vanishes after spin averaging. On the other hand, the scattering amplitude following from  $\mathcal{L}_{WZ}^{(2\gamma)}$  interferes only with the magnetic part of the Born amplitude, so that apart from kinematical factors the unpolarized elastic electron-nucleon cross section has the general structure

$$\frac{d\sigma}{d\Omega} \propto G_E^2(Q^2)(1 + \cos \Theta) + G_M^2(Q^2)\tau(3 - \cos \Theta) + G_M(Q^2)F_{WZ}^{(2\gamma)}(Q^2)\tau^2 \quad (25)$$

with Lorentz invariant  $\tau = Q^2/(4M^2)$  and electron scattering angle  $\Theta$  in the Breit frame. The form factor  $F_{WZ}^{(2\gamma)}(Q^2)$  is of the order of the e.m. coupling constant  $\alpha$ , and involves a loop integral and Fourier transforms of soliton profiles. Due to its origin from the Wess-Zumino action, it is parameterfree. In terms of the Lorentz invariant

$$\epsilon = \frac{1 + \cos \Theta}{3 - \cos \Theta} \quad (26)$$

the cross section then is given by

$$\frac{d\sigma}{d\Omega} \propto \frac{4\tau}{1 + \epsilon} \left( G_M^2(Q^2) + \frac{\epsilon}{\tau} G_E^2(Q^2) + \frac{\tau}{4}(1 + \epsilon)G_M(Q^2)F_{WZ}^{(2\gamma)}(Q^2) \right). \quad (27)$$

This is an interesting result, because it shows that the linear  $\epsilon$ -dependence is maintained, but the form factors  $\tilde{G}_{E,M}$  extracted through a Rosenbluth separation from this cross section are related to the single-photon-exchange form factors  $G_{E,M}$  by

$$\tilde{G}_M^2 = G_M^2 + \frac{\tau}{4} G_M F_{WZ}^{(2\gamma)} \quad (28)$$

$$\tilde{G}_E^2 = G_E^2 + \frac{\tau^2}{4} G_M F_{WZ}^{(2\gamma)}. \quad (29)$$

Evidently, with increasing  $Q^2$ , the extracted electric form factor  $\tilde{G}_E$  gets increasingly dominated by  $G_M$ ; even more so, if, as we have seen previously, the single-photon-exchange  $G_E$  passes through zero.

The author is very much indebted to H. Walliser and H. Weigel for numerous discussions.

- 
- [1] G. Holzwarth, Proc. 6th Int. Symp. Meson-Nucleon Phys.,  $\pi N$  Newsletter **10** (1995) 103.
  - [2] G. Holzwarth, Z. Phys. **A356** (1996) 339.
  - [3] E. Braaten, S.M. Tse and C. Willcox, Phys. Rev. **D34** (1986) 1482; Phys. Rev. Lett. **56** (1986) 2008.
  - [4] O. Kaymakalan and J. Schechter, Phys. Rev. **D 31** (1985) 1109; M. Bando, T. Kugo, S Uehara, K. Yamawaki, and T. Yanagida, Phys. Rev. Lett. **54** (1985) 1215.
  - [5] U.G. Meissner, N. Kaiser and W. Weise, Nucl. Phys. **A466** (1987) 685; U.G. Meissner, Phys. Reports **161** (1988) 213.
  - [6] B. Schwesinger, H.Weigel, G.Holzwarth, and A. Hayashi, Phys. Reports **173** (1989) 173.
  - [7] F. Meier, in: Baryons as Skyrme solitons, ed. G. Holzwarth (World Scientific, Singapore 1993), 159.
  - [8] V.A. Matveev, R.M. Muradyan, and A.N. Tavkhelidze, Lett. Nuovo Cim. **7** (1973) 719.
  - [9] A.L. Licht and A. Pagnamenta, Phys. Rev. **D 2** (1976) 1150 ; and 1156.
  - [10] X. Ji, Phys. Lett. **B254** (1991) 456.
  - [11] A. N. Mitra and I. Kumari, Phys. Rev. **D 15** (1977) 261.
  - [12] J.J. Kelly, Phys. Rev. **C 66** (2002) 065203
  - [13] F. Meier and H. Walliser, Phys. Reports **289** (1997) 383.
  - [14] H. Walliser, private communication.
  - [15] G. Höhler et al., Nucl. Phys. **B114** (1976) 505.
  - [16] A.F. Sill et al., Phys. Rev. **D48** (1993) 29.
  - [17] L. Andivahis et al., Phys. Rev. **D50** (1994) 5491.
  - [18] R.C. Walker et al., Phys. Rev. **D49** (1994) 5671.
  - [19] M. K. Jones et al., Phys. Rev. Lett. **84** (2000) 1398.
  - [20] O. Gayou et al., Phys. Rev. Lett. **88** (2002) 092301.
  - [21] M. Ostrick et al., Phys. Rev. Lett. **83** (1999) 276.
  - [22] M. Meyerhoff et al., Phys. Lett. **B327** (1994) 201.
  - [23] J. Becker et al., Eur. Phys. J. **A6** (1999) 329.
  - [24] D. Rohe et al., Phys. Rev. Lett. **83** (1999) 4257.
  - [25] R. Schiavilla, and I. Sick, Phys. Rev. **C64** (2001) 041002-1.
  - [26] R. Glazier et al., Eur.Phys.J. **A24** (2005) 101.
  - [27] R. Madey et al., Phys. Rev. Lett. **91** (2003) 122002.
  - [28] S. Rock et al., Phys. Rev. Lett. **49** (1982) 1139.
  - [29] A. Lung et al., Phys. Rev. Lett. **70** (1993) 718.
  - [30] H. Anklin et al., Phys. Lett. **B336** (1994) 313.
  - [31] H. Anklin et al., Phys. Lett. **B428** (1998) 248.



- [32] G. Kubon, H. Anklin et al. Phys. Lett. **B524** (2002) 26.
- [33] W. Xu et al., Phys. Rev. Lett. **85** (2000) 2900.
- [34] W. Xu et al., Phys. Rev. **C67** (2003) 012201 R.
- [35] G. Holzwarth, arXiv:hep-ph/0201138 (unpublished).
- [36] Jefferson Lab experiment E94-017, Spokespersons: W. Brooks and M. Vineyard.
- [37] G. Simon, F. Borkowski, C. Schmitt, and V. H. Walther, Z. Naturforsch. **35A** (1980) 1.
- [38] I.A. Qattan et al., Phys. Rev. Lett. **94** (2005) 142301.